Photoelectron Photoion Coincidence Spectroscopy of NCl_3 and NCl_2

Marius Gerlach,[a] Sophie Monninger,[a] Domenik Schleier,[a] Patrick Hemberger,[b] James T. Goettel,[c] Holger Braunschweig,[c] and Ingo Fischer*[a]

In Memoriam Siegfried Hünig.

We investigate NCl_3 and the NCl_2 radical by photoelectron-photoion coincidence spectroscopy using synchrotron radiation. The mass selected threshold photoelectron spectrum (ms-TPES) of NCl_3 is broad and unstructured due to the large geometry change. An ionization energy of 9.7 ± 0.1 eV is estimated from the spectrum and supported by computations. NCl_2 is generated by photolysis at 213 nm from NCl_3 and its ms-TPES shows an extended vibrational progression with a 90 meV spacing that is assigned to the symmetric N–Cl stretching mode in the cation. An adiabatic ionization energy of 9.94 ± 0.02 eV is determined.

The chemistry of NCl_3 is of interest in environmental chemistry because it is formed in wastewater treatment with hypochlorite. Due to its high volatility, it can act as a respiratory irritant in indoor air,[1] including pools.[2] Its strong UV absorption suggests that its photochemistry might be relevant for tropospheric chemistry as well. Furthermore, the molecule is also considered for use in chemical lasers.[3] From the inorganic chemistry point of view, chloramines are of interest as a versatile reagent, and because of the low polarity of the N–Cl bond.[4] Note that the electronegativities of N and Cl are almost identical.

As NCl_3 is explosive and difficult to handle in pure form,[5] little information is available on the compound. Geometries were obtained from microwave spectroscopy.[6] Photoelectron spectra of chloramines have been reported, but bands were mostly broad and structureless.[7] Griffiths *et al.* demonstrated that the decomposition of NCl_3 is photosensitized by Cl_2.[8] The NCl_3 photodissociation itself was investigated at 193 nm and 249 nm.[9] While the former wavelength preferentially produced NCl (a $^1\Delta$) + Cl_2, the latter led to NCl_2 + Cl. NCl_2, the main UV photoproduct, has been studied computationally,[10] but even less experimental work on this radical is available, apart from a UV/Vis absorption spectrum recorded in a microwave discharge[11] and a matrix IR spectrum.[12] This lack of spectroscopic data motivated us to study the photoionization of NCl_3 and NCl_2 utilizing vacuum ultraviolet (VUV) synchrotron radiation, which is an excellent tool to derive ionization (IE) and appearance energies (AE).[13] NCl_3 was introduced as a 20% solution with dichloromethane, while NCl_2 was produced by photolysis of NCl_3 in a side-sampled flow reactor.[14]

Photoelectron spectroscopy of reactive molecules suffers often from signals due to side products that impede assignments. We therefore employ photoelectron-photoion coincidence spectroscopy (PEPICO), which permits to record photoion mass-selected threshold photoelectron spectra (ms-TPES) for each species by correlating ions and electrons. While the majority of work used fluorine discharges[15] or pyrolysis[13,16] to generate reactive species, PEPICO has increasingly been combined with photolysis,[17] which expands the range of available species and gives in addition access to kinetics data.

The $Ar/NCl_3/CH_2Cl_2$ mixture was introduced into the experimental chamber via a flow reactor with a 300 μm hole. The photolysis laser beam propagates along the reactor axis and excited the sample at 213 nm. Radicals are generated along the reactor volume and effusively leak into the ionization volume of the PEPICO spectrometer, where they are ionized by VUV radiation. Due to collisions with the Ar bath gas, NCl_2 is at room temperature. The resulting photoions and electrons are detected in coincidence. To determine experimental conditions, photoionization mass spectra (PI-MS) were recorded with and without the photolysis laser. The resulting spectra, recorded at 10.5 eV photon energy, are shown in Figure 1. The upper trace depicts the PI-MS without photolysis. Intense peaks are observed at *m/z* 119, 121 & 123, with a minor peak at *m/z* 125, which correspond to the expected intensity of the NCl_3 isotopic pattern of 100:97:31:3. A signal at *m/z* 3 might be assigned to a H_3^+ fragment ion, but the peak shape suggests that it is more likely due to electronic noise. Although the laser is off, a small signal around *m/z* 84/86/88 is present. It is likely due to CH_2Cl_2, which is ionized by residual higher harmonics of the synchrotron light that were able to pass the gas filter. Note that CH_2Cl_2

[a] *M. Gerlach, S. Monninger, D. Schleier, Prof. Dr. I. Fischer*
Institute of Physical and Theoretical Chemistry, University of Würzburg
Am Hubland, 97074 Würzburg, Germany
E-mail: ingo.fischer@uni-wuerzburg.de
[b] *Dr. P. Hemberger*
Laboratory for Synchrotron Radiation and Femtochemistry, Paul Scherrer Institut (PSI)
5232 Villigen, Switzerland
[c] *Dr. J. T. Goettel, Prof. Dr. H. Braunschweig*
Institute of Inorganic Chemistry and Institute for Sustainable Chemistry and Catalysis with Boron, University of Würzburg
Am Hubland, 97074 Würzburg, Germany

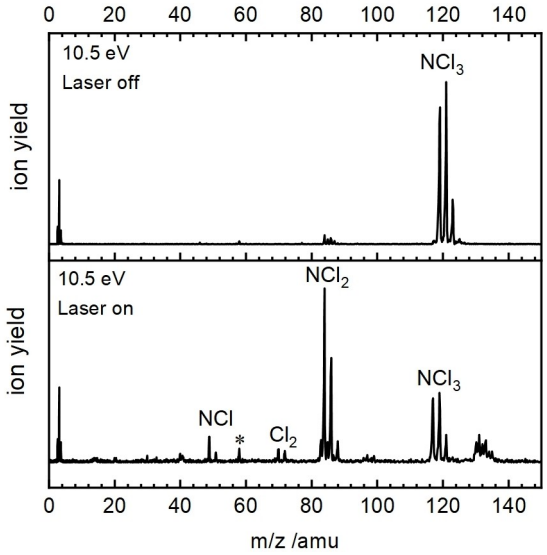

Figure 1. Photoionization mass spectra at 10.5 eV. Upper trace: The intense peaks at m/z = 119 to 121 correspond to NCl_3. Lower trace: With 213 nm photolysis, the NCl_3 signal decreases and peaks due to NCl_2 (m/z = 84 to 88) and NCl (m/z = 49 & 51) increase. The asterisk indicates residual acetone.

has the same *m/z* as NCl_2, but cannot be ionized by the fundamental radiation, because the first observable transition into the $A^{+2}B_2$ state lies at 11.317 eV .[18]

The lower trace shows the PI-MS with active photolysis laser. The dominant signal is now a group of three peaks at m/z 84,86 & 88, which corresponds well to the isotopic distribution of NCl_2 with relative intensities of 100:64:10. A small amount of NCl is also present at m/z 49 & 51, as concluded from the 3:1 intensity ratio. Additional peaks are due to residual acetone at m/z = 58 and Cl_2 at m/z 70 & 72. The IE of Cl_2 is 11.48 eV and thus above the 10.5 eV photon energy employed. Again, it is ionized by residual higher harmonics of the synchrotron light. Another group of peaks appear between m/z 130 and 135 but cannot be reasonably assigned.

The ms-TPES of the $X^{+2}A_2'' \leftarrow X\ ^1A_1$ transition of NCl_3, averaged over m/z = 119, 121 and 123 is shown in Figure 2. A broad band with an onset at around 9.7 eV and a maximum at 10.44 eV is observed, in agreement with previous work that reported a band maximum of 10.69 ± 0.02 eV and assigned the onset of the signal at 10.12 ± 0.1 eV to the adiabatic IE_{ad}.[7b] As a neutral molecule, NCl_3 has a pyramidal geometry (C_{3v}), while the cation is planar (D_{3h}). Thus, the broad spectrum reflects the large geometry change upon ionization and agrees with previous work, although onset and maximum are shifted to slightly lower energies. Strong activity in the umbrella mode is expected, but the low computed wavenumber of 125 cm^{-1}, small Franck-Condon factors close to threshold and overlap of the overtones in particular with hot- and sequence band transitions prevents spectral resolution. Pronounced features roughly 40 to 50 meV (320–400 cm^{-1}) apart are visible between 10.4 eV and 10.7 eV. An in-plane bending mode of NCl_3^+ was computed at 308 cm^{-1} but based on the computed geometries no activity is expected. An assignment to autoionizing resonances is thus more likely. The other vibrations of the cation were computed at 193 cm^{-1}, 516 cm^{-1} and 911 cm^{-1}. Calculations on the G4 level yielded an IE_{ad} = 9.67 eV. This agrees with Milburn *et al.* who computed the structures and energies of neutral, cationic, and anionic NH_mCl_n (m + n = 1, 2 or 3)[19] and found IE_{ad} = 9.81 eV on the MP2 level of theory. Franck-Condon simulations did not yield a fit that allows to extract a reliable IE. From the onset of the signal we therefore estimate an IE of 9.7 ± 0.1 eV, in reasonable agreement with theory. Note that the origin transition might be unobservable due to small Franck-Condon factors and thus appear below the signal onset.

As noted above, no prior experimental data are available for the photoionization of NCl_2. CCSD(T) calculations with an aug-cc-pVDZ basis set indicate an IE_{ad} = 9.94 eV for the $X^{+1}A_1 \leftarrow X^2B_1$ transition, while G4 yielded a slightly higher value of 9.98 eV. Both agree with the previously computed value of 9.90 eV.[19] As shown in Figure 1, an excellent conversion is achieved for the photolysis to NCl_2. The ms-TPES averaged over *m/z* 84, 86 and 88 is presented in Figure 3. A rather regular progression of nine bands is observed, separated by 0.09 eV (730 cm^{-1}), with the origin transition at 9.94 eV. On the high energy side of each band, small shoulders are visible. At higher vibrational excitation the peaks appear to broaden and become less regular above 10.6 eV, see below.

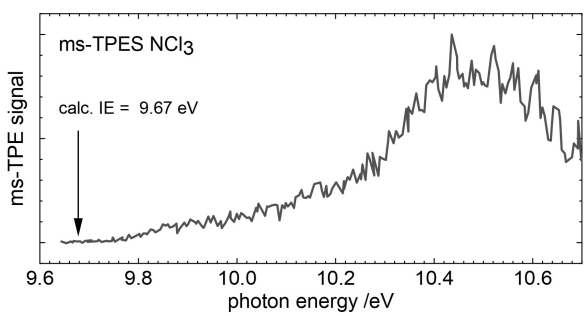

Figure 2. ms-TPES of NCl_3. The spectrum features a broad band. While an adiabatic ionization energy of 9.67 eV was calculated, an experimental IE of 9.7 ± 0.1 eV is estimated from the signal onset.

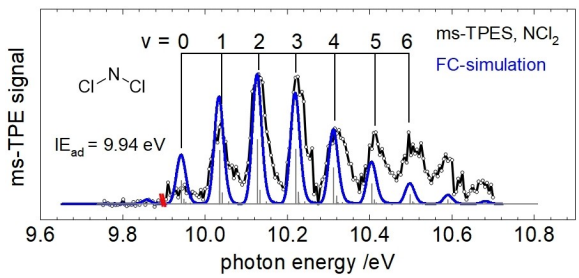

Figure 3. ms-TPES of NCl_2. The black line shows the experimental spectrum. The simulation (blue) is obtained by convoluting the computed stick spectrum (grey) with a Gaussian. From the simulation an IE_{ad} of 9.94 eV is determined, which is the exact value obtained from CCSD(T) computations. The red dash separates two different scans.

To assign the vibrational structure, a Franck-Condon simulation was carried out using ezSpectrum.[20] It was based on the CCSD(T)/aug-cc-pVDZ geometries given in Table 1, which summarizes the relevant geometry parameters. For comparison, the values computed at the B3LYP//6-31G(2df,p) level of theory are also given. As visible, both the bond length R_{N-Cl} and the bond angle θ changes upon ionization. R_{N-Cl} exhibits a dramatic decrease of almost 0.1 Å and causes the pronounced progression. The computed stick spectrum (grey sticks) was convoluted by a Gaussian and yielded the simulation depicted in blue. The best agreement between the experimental and simulated spectrum was obtained by shifting the computed spectrum with the 0–0 transition to 9.94 ± 0.02 eV, which corresponds to the IE_{ad}. The error was estimated from the full width at half maximum (fwhm) of the bands.

For the three vibrational modes of the cation, wavenumbers of 746 cm^{-1} (symmetric stretch ν_1), 365 cm^{-1} (bending mode ν_2) and 837 cm^{-1} (asymmetric stretch ν_3) were computed. As expected from the large reduction in bond length upon ionization, the simulation predicts a progression in ν_1 , which can be recognized in the spectrum up to 6th or 7th overtone. Each transition is accompanied by another smaller transition on the high energy side. According to the simulation they are assigned to a combination of ν_1 with a ν_2 sequence band or overtone, i.e. transitions of the type $1_0^n 2_1^1$ as well as $1_0^n 2_0^1$. Overall excellent agreement between the experimental spectrum and the simulation is achieved. Only for highly excited overtones deviations become visible, either due to anharmonicity or due to the appearance of Fermi resonances, which might also explain the apparent broadening and splitting at higher energies.

The large decrease of R_{N-Cl} upon ionization can easily be explained within the VSEPR (valence shell electron pair repulsion) model. Donation of electron density from the Cl atoms to the empty p-orbital on the N leads to a resonance stabilization of the positive charge and a partial N=Cl double-bond character of the ion. This has also been concluded more quantitatively in previous high-level *ab initio* computations.[19] The TPES in Figure 3 thus illustrates nicely the success of this simple approach. Furthermore, the computations show that the SOMO (singly occupied molecular orbital) has antibonding character along the N–Cl bond, therefore R_{N-Cl} decreases upon ionization. Due to this shorter N–Cl bonds, the repulsion between the chlorine atoms increases and consequently the cations' $\theta_{Cl\text{-}N\text{-}Cl}$ angle increases by 6.3°.

To summarize, NCl_3 and NCl_2 have been investigated using threshold photoelectron photoion coincidence spectroscopy. NCl_3 shows a broad and undefined spectrum, due to the large geometry change from C_{3v} to D_{3h} and the low wavenumber of the cationic umbrella mode of 125 cm^{-1}. An ionization energy of 9.7 ± 0.1 eV is estimated, in agreement with the computed IE of 9.67 eV. The photoion mass-selected threshold photoelectron spectrum of the NCl_2 radical features a strong progression in the symmetric stretching mode of the cation. The significant reduction of the N–Cl bond length by more than 0.1 Å and increase of the $\theta_{Cl\text{-}N\text{-}Cl}$ angle can be rationalized by the antibonding character of the SOMO in the neutral and the resonance stabilization of the positive charge in the cation. An adiabatic ionization energy of 9.94 ± 0.02 eV was determined.

Table 1. Computed geometries of NCl_2 and NCl_2^+

	Neutral NCl_2		Cationic NCl_2	
	DFT	CCSD(T)	DFT	CCSD(T)
R_{N-Cl}/Å	1.716	1.747	1.619	1.654
$\theta_{Cl\text{-}N\text{-}Cl}$	110.9°	109.6°	117.2°	115.5°

Experimental Section

The experiments were performed at the VUV beamline of the Swiss Light source (SLS), using the double imaging CRF-PEPICO spectrometer.[21] As neat NCl_3 is explosive, but solutions are safe to handle,[22] a 20% solution in CH_2Cl_2 was employed. NCl_3 was synthesized according to the procedure by Noyes,[23] but instead of traditional glassware, a FEP (fluorinated ethylene-propylene copolymer) tube and a PTFE container were used. The solution was dried over sodium sulphate and decanted over P_2O_5. During the experiments, it was kept at 20 °C to ensure a constant concentration in the gas phase. An argon flow was passed over the sample (1 bar). The sample gas mixture was introduced into a 1.25 cm O.D. quartz tube photolysis reactor mounted parallel to the synchrotron beam.[14] The $Ar/NCl_3/CH_2Cl_2$ sample flow into the reactor was adjusted by a mass flow controller (MFC). A second MFC connected to pure argon employed as buffer gas allowed adjustment of the reactor pressure. For photolysis, the 5th harmonic of a 10 Hz Nd:YAG laser (~25 mJ) was employed. The sample leaves the reactor tube through a 300 μm hole and is ionized by the synchrotron light. The resulting photoelectrons and photoions are accelerated in opposite directions by a constant extraction field of 213 $V\,cm^{-1}$. Both are detected by Roentdek DLD40 position-sensitive delay-line detectors. Photoelectron-photoion coincidences are detected in a multiple-start/multiple-stop data acquisition scheme.[24] The photon energy was calibrated using the Ar 11 s' to 14 s' autoionization transitions in both the first and second order. A 150 l/mm grating was used. Ionization energies are corrected for the Stark-shift (+ 11 meV) at an extraction field of 213 $V\,cm^{-1}$. The VUV photon energy was scanned from 9.6 to 10.7 eV in 5 meV steps to record the ms-TPES of NCl_3. For the ms-TPES of NCl_2 the photon energy was scanned with a step size of 5 meV. Additional scans between 9.75 eV and 9.90 eV showed no further bands. Higher harmonic radiation of the synchrotron light was eliminated by a gas filter, operating with a mixture of argon and helium. The contribution of hot electrons was removed by the procedure given by Sztáray *et al.*[25] Quantum chemical calculations were performed either at the G4 level of theory or by coupled cluster theory (CCSD(T)), using the Gaussian 09 suite of programmes.[26] Minimum energy structures were confirmed by the Hessian calculations that yielded only real vibrational frequencies. Franck-Condon simulations based on the CCSD(T) results were carried out employing ezSpectrum.[20]

Acknowledgements

The experiments were performed at the VUV beamline of the Swiss Light Source, located at the Paul Scherrer Institute (PSI). The work was financially supported by the Deutsche Forschungsgemeinschaft (DFG), contract FI575/13-2. It was also supported by the Swiss Federal Office for Energy (BFE Contract Number SI/501269-01). J.T.G. acknowledges the Government of Canada for a Banting

Fellowship and the Alexander von Humboldt Foundation for financial support. We thank Lea Bosse for providing artwork for the Table of Contents graphic. Open Access funding enabled and organized by Projekt DEAL.

Conflict of Interest

The authors declare no conflict of interest.

Keywords: radicals · photoelectron spectroscopy · synchrotron radiation · nitrogen trichloride · photolysis

[1] J. M. Mattila, P. S. J. Lakey, M. Shiraiwa, C. Wang, J. P. D. Abbatt, C. Arata, A. H. Goldstein, L. Ampollini, E. F. Katz, P. F. DeCarlo, S. Zhou, T. F. Kahan, F. J. Cardoso-Saldana, L. H. Ruiz, A. Abeleira, E. K. Boedicker, M. E. Vance, D. K. Farmer, *Environ. Sci. Technol.* **2020**, *54*, 1730–1739.
[2] N. Massin, A. B. Bohadana, P. Wild, M. Hery, J. Toamain, G. Hubert, *Occup. Environ. Med.* **1998**, *55*, 258–263.
[3] T. Masuda, T. Nakamura, M. Endo, T. Uchiyama, *Jpn. J. Appl. Phys.* **2009**, *48*, 5.
[4] P. Kovacic, M. K. Lowery, K. W. Field, *Chem. Rev.* **1970**, *70*, 639–665.
[5] C. Wentrup, *Aust. J. Chem.* **2019**, *72*, 585–594.
[6] G. Cazzoli, P. G. Favero, A. Dalborgo, *J. Mol. Spectrosc.* **1974**, *50*, 82–89.
[7] a) A. W. Potts, H. J. Lempka, D. G. Streets, W C. Price, *Philos. Trans. R. Soc. London* **1970**, *268*, 59–76; b) D. Colbourne, D. C. Frost, C. A. McDowell, N. P. C. Westwood, *J. Chem. Phys.* **1978**, *69*, 1078–1085.
[8] J. G. A. Griffiths, R. G. W. Norrish, T. M. Lowry, *Proc. Roy. Soc. A* **1931**, *130*, 591–609.
[9] R. D. Coombe, J. V. Gilbert, S. S. Beaton, N. Mateljevic, *J. Phys. Chem. A* **2002**, *106*, 8422–8426.
[10] A. Papakondylis, A. Mavridis, A. Metropoulos, *J. Phys. Chem.* **1995**, *99*, 10759–10765.
[11] T. C. Clark, M. A. A. Clyne, *Trans. Faraday Soc.* **1969**, *65*, 2994–3004.
[12] C. K. Kohlmiller, L. Andrews, *Inorg. Chem.* **1982**, *21*, 1519–1522.
[13] a) P. Hemberger, Z. Pan, A. Bodi, J. A. van Bokhoven, T. K. Ormond, G. B. Ellison, N. Genossar, J. H. Baraban, *ChemPhysChem* **2020**, *21*, 2217–2222; b) M. Steglich, V. B. F. Custodis, A. J. Trevitt, G. Dasilva, A. Bodi, P. Hemberger, *J. Am. Chem. Soc.* **2017**, *139*, 14348–14351; c) D. P. Mukhopadhyay, D. Schleier, S. Wirsing, J. Ramler, D. Kaiser, E. Reusch, P. Hemberger, T. Preitschopf, I. Krummenacher, B. Engels, I. Fischer, C. Lichtenberg, *Chem. Sci.* **2020**, *11*, 7562–7568.
[14] D. L. Osborn, P. Zou, H. Johnsen, C. C. Hayden, C. A. Taatjes, V. D. Knyazev, S. W. North, D. S. Peterka, M. Ahmed, S. R. Leone, *Rev. Sci. Instrum.* **2008**, *79*, 104103.
[15] a) J. M. Dyke, *Phys. Chem. Chem. Phys.* **2019**, *21*, 9106–9136; b) G. A. Garcia, X. Tang, J.-F. Gil, L. Nahon, M. Ward, S. Batut, C. Fittschen, C. A. Taatjes, D. L. Osborn, J.-C. Loison, *J. Chem. Phys.* **2015**, *142*, 164201; c) D. Schleier, A. Humeniuk, E. Reusch, F. Holzmeier, D. Nunez-Reyes, C. Alcaraz, G. A. Garcia, J. C. Loison, I. Fischer, R. Mitric, *J. Phys. Chem. Lett.* **2018**, *9*, 5921–5925.
[16] a) T. Schüßler, H.-J. Deyerl, S. Dümmler, I. Fischer, C. Alcaraz, M. Elhanine, *J. Chem. Phys.* **2003**, *118*, 9077–9080; b) E. Reusch, F. Holzmeier, P. Constantinidis, P. Hemberger, I. Fischer, *Angew. Chem. Int. Ed.* **2017**, *56*, 8000–8003; *Angew. Chem.* **2017**, *129*, 8113–8116.
[17] a) K. Voronova, K. M. Ervin, K. G. Torma, P. Hemberger, A. Bodi, T. Gerber, D. L. Osborn, B. Sztaray, *J. Phys. Chem. Lett.* **2018**, *9*, 534–539; b) D. Schleier, P. Constantinidis, N. Faßheber, I. Fischer, G. Friedrichs, P. Hemberger, E. Reusch, B. Sztaray, K. Voronova, *Phys. Chem. Chem. Phys.* **2018**, *20*, 10721–10731; c) D. Schleier, E. Reusch, M. Gerlach, T. Preitschopf, D. P. Mukhopadhyay, N. Fassheber, G. Friedrichs, P. Hemberger, I. Fischer, *Phys. Chem. Chem. Phys.* **2021**, *23*, 1539–1549; d) D. Schleier, E. Reusch, L. Lummel, P. Hemberger, I. Fischer, *ChemPhysChem* **2019**, *20*, 2413–2416.
[18] R. Tuckett, J. Harvey, P. Hemberger, A. Bodi, *J. Mol. Spectrosc.* **2015**, *315*, 172–183.
[19] R. K. Milburn, C. F. Rodriquez, A. C. Hopkinson, *J. Phys. Chem. B* **1997**, *101*, 1837–1844.
[20] S. Gozem, A. I. Krylov, "The ezSpectra suite: An easy-to-use toolkit for spectroscopy modeling", WIRES CMS, e1546 (**2021**).
[21] B. Sztaray, K. Voronova, K. G. Torma, K. J. Covert, A. Bodi, P. Hemberger, T. Gerber, D. L. Osborn, *J. Chem. Phys.* **2017**, *147*, 013944.
[22] W. Hentschel, *Ber. Dtsch. Chem. Ges.* **1897**, *30*, 1434–1437.
[23] W. A. Noyes, G. H. Coleman, G. E. Goheen, in *Inorg. Synth.*, **1939**, pp. 65–67.
[24] A. Bodi, B. Sztáray, T. Baer, M. Johnson, T. Gerber, *Rev. Sci. Instrum.* **2007**, *78*, 084102.
[25] B. Sztáray, T. Baer, *Rev. Sci. Instrum.* **2003**, *74*, 3763–3768.
[26] Gaussian 09, Revision E.01, M. J. Frisch, G. W. Trucks, H. B. Schlegel, G. E. Scuseria, M. A. Robb, J. R. Cheeseman, G. Scalmani, V. Barone, B. Mennucci, G. A. Petersson, H. Nakatsuji, M. Caricato, X. Li, H. P. Hratchian, A. F. Izmaylov, J. Bloino, G. Zheng, J. L. Sonnenberg, M. Hada, M. Ehara, K. Toyota, R. Fukuda, J. Hasegawa, M. Ishida, T. Nakajima, Y. Honda, O. Kitao, H. Nakai, T. Vreven, J. A. Montgomery, J. E. Peralta, F. Ogliaro, M. Bearpark, J. J. Heyd, E. Brothers, K. N. Kudin, V. N. Staroverov, T. Keith, R. Kobayashi, J. Normand, K. Raghavachari, A. Rendell, J. C. Burant, S. S. Iyengar, J. Tomasi, M. Cossi, N. Rega, J. M. Millam, M. Klene, J. E. Knox, J. B. Cross, V. Bakken, C. Adamo, J. Jaramillo, R. Gomperts, R. E. Stratmann, O. Yazyev, A J. Austin, R. Cammi, C. Pomelli, J. W. Ochterski, R. L. Martin, K. Morokuma, V. G. Zakrzewski, G. A. Voth, P. Salvador, J. J. Dannenberg, S. Dapprich, A. D. Daniels, O. Farkas, J. B. Foresman, J. V. Ortiz, J. Cioslowski, D. J. Fox, Gaussian, Inc., Wallingford CT, **2013**.

Manuscript received: July 16, 2021
Revised manuscript received: August 10, 2021
Accepted manuscript online: August 14, 2021
Version of record online: August 26, 2021